(Received 17 November 2025, Accepted 6 January 2026, Scheduled 4 February 2026)

A Self-Diplexing Multi-Mode SIW Cavity-Backed Antenna with a Lambda (λ)-Shaped Slot for X- and Ku-Band Applications

Ravindiran Asaithambi[1,*], Maruthamuthu P. Prabakaran[2], and Govindasamy Rajesh[3]

[1] *Department of Electronics and Communication Engineering, Sri Ramachandra Faculty of Engineering and Technology (SRET) Sri Ramachandra Institute of Higher Education and Research, Chennai, India*
[2] *Department of Electronics and Communication Engineering, A. K. T Memorial College of Engineering and Technology Kallakurichi, Tamilnadu, India*
[3] *Department of Electronics and Communication (Advanced Communication Technology) R. M. K. Engineering College (Autonomous), Kavaraipettai Chennai, India*

ABSTRACT: This paper presents a self-diplexing, multi-mode substrate-integrated waveguide (SIW) antenna based on a cavity-backed SIW configuration. The antenna employs a λ-shaped radiating slot that provides inherent filtering characteristics. The proposed architecture achieved independent dual-band control through two diagonally oriented slots arranged at 45°, forming a λ-shaped aperture. These slots, integrated within an SIW cavity and excited by two separate 50-Ω microstrip feeds, enable dual resonances at 10.76 GHz and 12.39 GHz, corresponding to the TE_{210} and TE_{220} modes for X-band and Ku-band operation, respectively. Experimental validation confirmed reflection coefficients below -10 dB in both bands, with measured bandwidths of 3.0% (10.61–10.93 GHz) and 3.2% (12.19–12.59 GHz). The proposed filtenna achieves gains of 6.12 dBi and 6.15 dBi and exhibits high port isolation exceeding 28 dB between channels, along with an overall simulated radiation efficiency of 91.16%. In addition, a single-layer structure offers two-band operation, broadside linear polarization, and intrinsic filtering functionality, making it a compact and efficient solution for X/Ku-band applications.

1. INTRODUCTION

Recent advancements in wireless communication systems have led to the increasing use of multiband antennas. However, the presence of multiple bands across several antennas poses significant challenges for achieving effective isolation between them. Additionally, owing to their single-port topology, only one mode is typically used for data transmission or reception [1, 2]. To enhance performance, various antenna concepts have been explored, including self-duplex, self-quadruplexing, self-triplexing, self-diplexing, and self-hexaplexing antennas for multiband operations [3]. Among them, self-diplexing antenna (SDA)-based multiband design has garnered considerable attention in modern wireless and satellite communication systems [4]. The self-diplexing concept features a self-tunable frequency, which contributes to cost reduction and compact antenna design [5]. Suitable for both half and full-duplex communication, the SDA is a relatively novel concept aimed at reducing additional power consumption.

In recent years, substrate integrated waveguide (SIW) technology has gained popularity for planar substrates owing to its high-quality factor, compact size, high gain, excellent radiation properties, and seamless integration with planar devices [6, 7]. Compared to other planar guiding structures, SIW antennas offer lower losses and superior radiation characteristics in compact, single configurations [8]. However, the primary drawback of SIW antennas is the increased cost of Radio Frequency (RF) module [9]. Integrating self-diplexing capabilities with SIW technology can improve performance while enhancing cost-effectiveness and compactness [10, 17]. Various antenna designs with different frequency variations have been reported in the literature, but some performance constraints persist.

To address these issues, this study proposes a self-diplexing multi-mode substrate-integrated waveguide antenna with SIW cavity backing featuring a Lambda (λ)-shaped radiating slot. In [11], an ultra-compact cavity-backed SDA was introduced using a shielded quarter-mode SIW to support Wireless Local Area Networks (WLAN) and Worldwide Interoperability for Microwave Access (WiMAX). In [25, 26], the design achieved isolation levels exceeding 40 dB between the ports; however, this performance was obtained at the expense of a larger physical footprint. Furthermore, no equivalent circuit model was provided to verify the simulation. In [12], a C-band SDA with two microstrip feed lines was designed to excite the fundamental mode, demonstrating superior performance compared to conventional SIW designs in experimental analysis.

The achieved performance may be unreliable because the functionality of the antenna has only been validated for C-band applications. In [13], a substrate integrated waveguide (SIW)-based self-triplexing antenna (STA) was proposed. The substrate integrated waveguide (SIW)-cavity was initially loaded with a hexagon-shaped slot and combined with a pair of rectangular transverse slots. The high isolation performance of the model established the triplexer antenna as a suitable option for applications in the C and X bands. However, the cir-

* Corresponding author: Ravindiran Asaithambi (ravigce2002@gmail.com).

cuit optimization process is time-consuming. In [14], a wide-band self-diplexing antenna utilizing SIW technology was introduced, with bandwidths controlled by stepped impedance specifications. The experimental results demonstrated better performance than the conventional models. However, the port-to-port isolation was limited to only 20.5 dB, which could impact the antenna's overall performance. Ref. [15] presented a low-profile, cost-effective, and efficient SIW-based STA for WiMAX and WLAN applications. The antenna reported in [15] operated at three distinct frequencies: 3.5 GHz, 4.8 GHz, and 5.4 GHz. Experimental assessments showed a high gain and efficiency compared to conventional designs, with a good match between the measured and simulated results. Higher Front-To-Back Ratio (FTBR) further enhances the performance of the presented model.

Existing antenna design research studies have certain limitations, outlined as follows:

I. Most existing methodologies focus on developing various antenna designs to enhance communication efficiency. However, no study has explored a Lambda (λ)-shaped radiating slot-based filtenna design.

II. A lambda (λ)-shaped radiating slot design significantly enhances the effectiveness of the designed filtenna.

III. The performance in [12] was deemed unreliable as the results were validated only for C-band applications (4.03–4.16 GHz and 4.81–5 GHz).

IV. In [14], the isolation between the ports was limited to 20.5 dB, which compromised the complete performance evaluation of the antenna design.

2. PROPOSED CONFIGURATION AND MODE ANALYSIS

2.1. Self Diplexing Filtenna Configuration

A. Figure 1 illustrates the 3D and top views of the proposed filtenna design, with final dimensions of $25 \times 19 \times 0.787\,\text{mm}^3$. The structure was built on Rogers RT/Duroid 5880 dielectric material, which is characterized by a dielectric constant of 2.20. The design features an SIW cavity resonator intended to accommodate F-shaped metallic vias, which function as shielding walls and effectively act as magnetic boundaries.

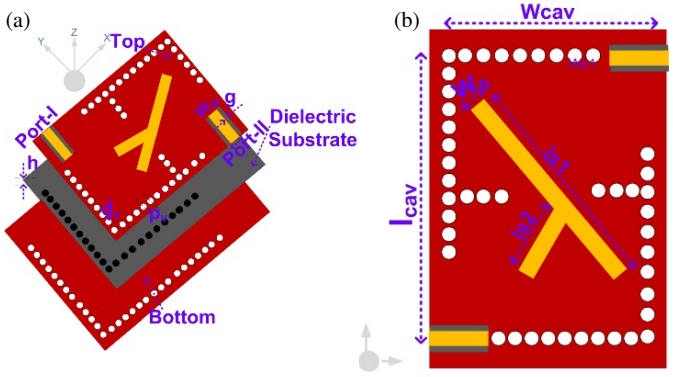

FIGURE 1. The proposed Lambda (λ)-shaped radiating slot-based filtenna design concerning (a) 3D view and (b) aerial view [$l_{cav} = 25$, $W_{cav} = 19$, $W_s = 2.6$, $l_{s1} = 13$, $l_{s2} = 6$, $d_v = 1.0$, $g = 0.9$, $t = 0.9$, $p_v = 1.5$, $w_{50} = 2.4$; unit: mm].

The proposed self-diplexing filtenna (SDF) operates in a multi-mode SIW (FMSIW) owing to the incorporation of a lambda (λ)-shaped slot and a pair of independent 50 Ω microstrip transmission feedlines located on opposite sides.

The resonance frequencies associated with the fundamental and higher-order resonant modes (TE_{mn0}) for the modified rectangular FMSIW cavity were calculated using the following formula [23, 24].

$$f_{mn0}^{\text{FMSIW}} = \frac{1}{2\pi\sqrt{\mu\varepsilon}}\sqrt{\left(\frac{m\pi}{L_{\text{effective}}^{\text{FMSIW}}}\right)^2 + \left(\frac{n\pi}{W_{\text{effective}}^{\text{FMSIW}}}\right)^2} \quad (1)$$

where $m = 1, 2, 3, \ldots$ and $n = 1, 2, 3, \ldots$ denote the number of half-cycle variations of the field along the x-axis and y-axis, respectively; $\varepsilon = \varepsilon_0\varepsilon_r$ and $\mu = \mu_0\mu_r$ denote the dielectric permittivity and magnetic permeability of the dielectric substrate.

The equivalent effective length and effective width are determined using the following equations:

$$L_{\text{effective}}^{\text{FMSIW}} = l_{\text{cavity}} - 1.08\frac{d_v^2}{p_v} + 0.1\frac{d_v^2}{l_{\text{cavity}}} \quad (2)$$

$$W_{\text{effective}}^{\text{FMSIW}} = w_{\text{cavity}} - 1.08\frac{d_v^2}{p_v} + 0.1\frac{d_v^2}{w_{\text{cavity}}} \quad (3)$$

Parameters w_{cav1} and l_{cav1} denote the width and length of the proposed modified rectangular FMSIW cavity resonator, respectively. Similarly, d_v represents the diameter, whereas p_v indicates the distance separating the adjacent vias.

B. To reduce energy leakage, it is advised to maintain conditions where the ratio of diameter to wavelength ($d_v/\lambda_0 = 1/25 = 0.04$ remains ≤ 0.1, and the ratio of diameter to pitch ($d_v/p_v = 1/1.5 = 0.66$) stays ≥ 0.5. Here, λ_0 represents the wavelength associated with the lowest resonance frequency of the dielectric material used. Due to the notably high aspect ratio of the proposed FMSIW, width-to-height, only specific TE_{mn0} modes are capable of resonating within the substrate integrated waveguide (SIW) resonator. The key parameters are designed to ensure that the TE_{210} mode is in operation within the target frequency range, as illustrated in Figure 2(a).

2.2. Eigen-Mode Analysis with and without Slot

C. To determine the mode configuration of the proposed SDF, an eigenmode solver in the Computer Simulation Technology Microwave Studio (CST MS) software was used, as illustrated in Figure 2 and Figure 3. Initially, an SIW structure with an SIW cavity, excluding the radiating slot, was analyzed using the eigenmode solver to examine the electric field distribution, as depicted in Figure 2. From Figure 2(a), it has been noted that the cavity without radiating slots supports FMSIW, with the TE_{210} and TE_{220} modes appearance at 11.51 GHz and 12.56 GHz, respectively, as seen in Figure 2(a) and Figure 2(b).

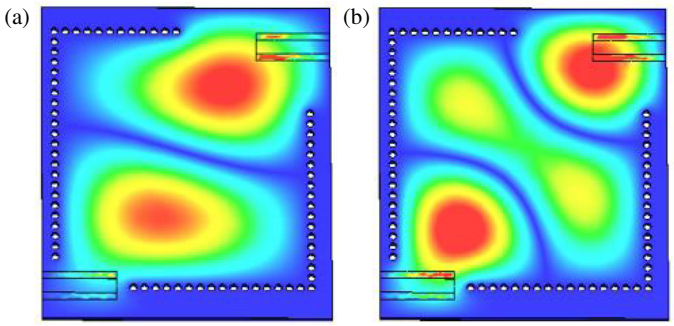

FIGURE 2. Distributions of electric fields at the original rectangular SIW cavity under eigenmode simulation. (a) TE_{210}. (b) TE_{220}.

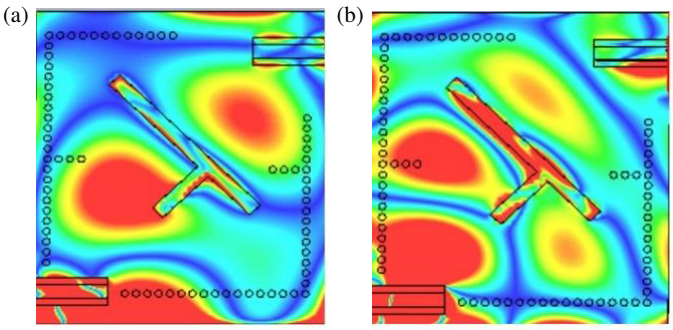

FIGURE 3. Distributions of electric fields a lambda (λ)-shaped slot rectangular SIW cavity under eigenmode simulation. (a) TE_{210}. (b) TE_{220}.

D. Subsequently, two slots — comprising diagonal slots — are introduced. To achieve optimal field disruption, the slot lengths were varied between $\lambda_0/4$ and $\lambda_0/2$, approximately one-fourth to half the wavelength, as shown in Figure 3. This cavity modification introduces additional inductive and capacitive effects, consequently altering the relevant resonant frequencies and modes. As a result, the TE_{210} and TE_{220} resonant frequencies shifted to 10.76 GHz and 12.39 GHz, respectively, as depicted in Figures 3(a) and 3(b).

E. Furthermore, Figure 3 reveals that owing to the symmetrical plane, the highest electric field intensities occur at specific points. Given the high SIW width-to-height ratio and the symmetrical plane of the proposed antenna, the magnetic field is aligned with the normal remains zero, allowing these planes in the SIW to be regarded as quasi-magnetic walls. The presence of the slot generates strong reactive loading, significantly affecting the TE_{220} mode.

2.3. Equivalent Circuit Model of SDF

F. An equivalent schematic was developed to illustrate the system, with slots incorporated to introduce additional capacitance, as depicted in Figure 4. A parallel-connected RLC circuit is utilized to depict all resonators, while a lambda (λ)-designed slot is modeled as a shunt capacitor. The first and second resonators were characterized by their respective resistance, inductance, and capacitances, denoted as R_{1pl}, L_{1pl}, C_{1pl} and R_{2pl}, L_{2pl}, C_{2pl}.

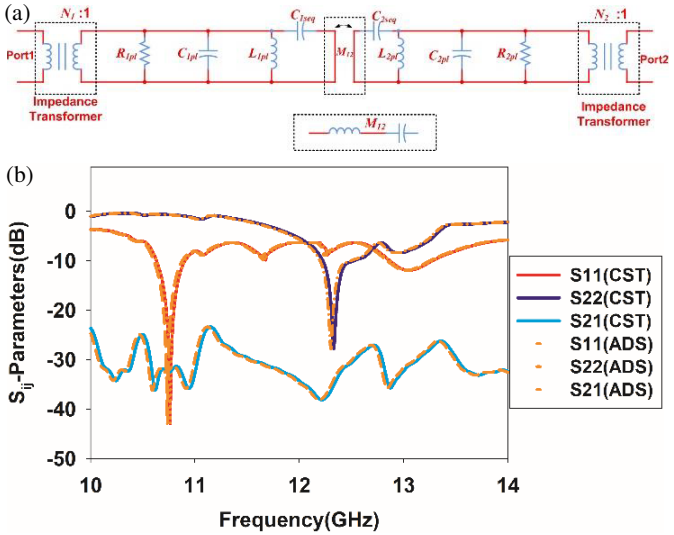

FIGURE 4. (a) Lumped element equivalent circuit model of the self-diplexing filtenna. (b) CST vs ADS.

Component	Value	Component	Value
R_{1pl}	100 kΩ	R_{2pl}	100 kΩ
L_{1pl}	15.12 nH	L_{2pl}	1.12 nH
C_{1pl}	0.071 pF	C_{2pl}	0.141 pF
C_{1seq}	0.068 pF	C_{2seq}	0.068 pF
L_{mn}	10.51 nH	N_1	0.356
C_{mn}	5.46 pF	N_2	0.396

These passive elements are connected in a shunt configuration to analyze the radiated patch values, while a lambda (λ)-shaped slot introduces shunt capacitances C_{1seq} and C_{2seq} associated with each port in the circuit diagram. N_1 and N_2 function as impedance transformers, ensuring impedance matching between the ports, that is the substrate integrated waveguide (SIW) cavities and microstrip lines. The mutual coupling among the pair resonators is illustrated by M_{12}, which is designed as a sequence connection of inductor (L_{mn}) and capacitor (C_{mn}).

The input impedance and resonance frequency of the resonators connected to port-1 and port-2 are given by:

$$f_{\text{reso}} = \frac{1}{2\pi\sqrt{L_P C_s}} \tag{4}$$

$$Z_{\text{input}} = \frac{j\omega_r L_P}{1-\omega_r^2 L_P C_s} \tag{5}$$

G. The resonance frequency is primarily influenced by cavity inductance (L_S) and slot capacitance (C_S), as indicated in Eq. (4). Notably, the capacitance (C_S) is directly dependent on slot dimensions. An increase in the slot size leads to a higher capacitance (C_S), which in turn shifts the resonance frequency to lower values.

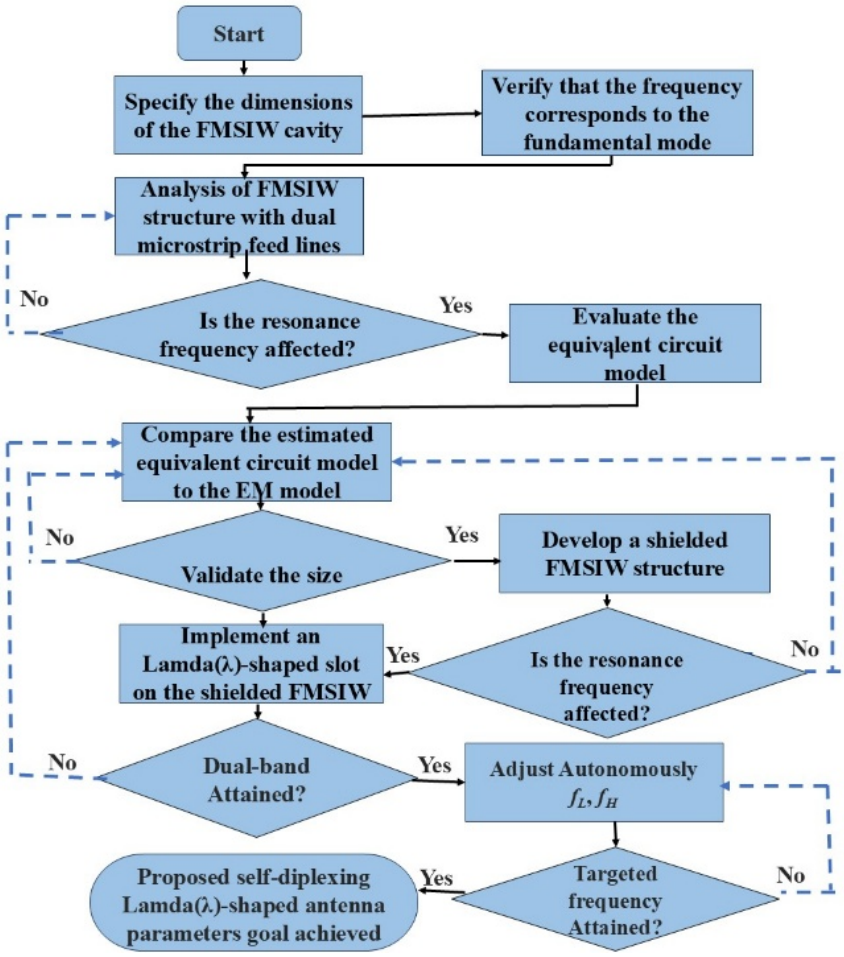

FIGURE 5. Flowchart diagram of the presented SDF.

2.4. Flowchart of Prototype SDF

The design is optimized to ensure the multi-mode operation of a lambda (λ)-shaped radiating slot, which consists of a combination of two diagonal slots. The design steps and antenna performance analysis are illustrated in the flowchart in Figure 5.

First, an SIW cavity was designed and constructed using CST MS software. The design parameters, including the width, length, and height of the SIW cavity, were calculated using Eqs. (1) to (3). Next, Eqs. (4) and (5) are applied to calculate the frequency of operation and input impedance matching, ensuring operation in the TE_{210} and TE_{220} modes. To develop the self-diplexing filtenna, two 50 Ω microstrip feed lines were incorporated to supply power to the proposed SIW cavity. Subsequently, an equivalent circuit with a lumped element model was constructed to predict the resonance frequencies.

Once the dimensions of the proposed geometry are finalized, the design is enclosed with FMSIW and centered with a lambda (λ)-shaped slot. Experimental validation and testing were also performed. If the designed filtenna meets the performance expectations, it is considered the final design and undergoes further performance analysis. Otherwise, the design parameters were reevaluated and adjusted accordingly. The rectangular SIW cavity operates at two distinct frequencies, 10.76 GHz and 12.39 GHz, making it suitable for X- and Ku-band applications.

3. PROPOSED DESIGN METHODOLOGY AND OPERATIONAL MECHANISM

This section discusses the various evaluation steps involved in the proposed self-diplexing filtenna design, as illustrated in Figure 6. The inherent filtering characteristics arise from the controlled excitation of cavity modes and slot coupling mechanism. The inherent filtering response is achieved through the selective excitation of distinct SIW cavity modes. These modes couple differently to the λ-shaped slot, enabling frequency-selective radiation. The first step focused on selecting the resonator shape. In this case, a rectangular shape was chosen and en-

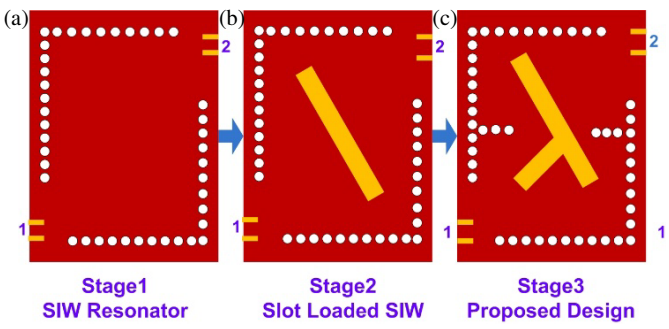

FIGURE 6. Different evaluation stages of the proposed filtenna.

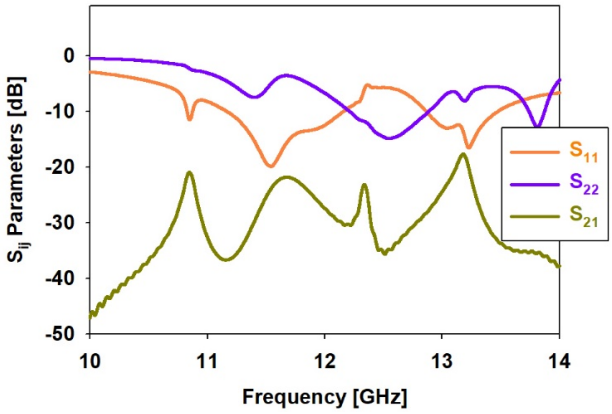

FIGURE 7. Stage 1, S_{ij} parameters.

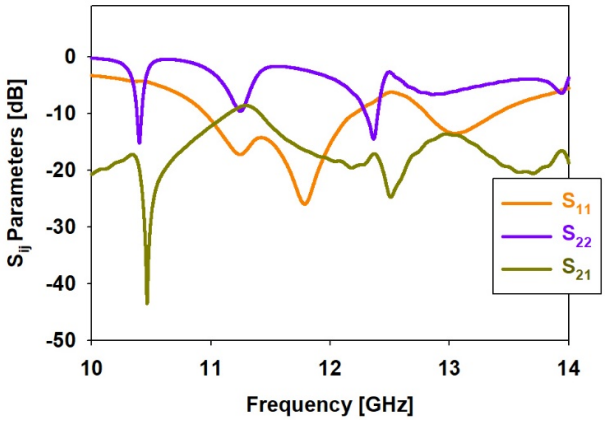

FIGURE 8. Stage 2, S_{ij} parameters.

closed with L-shaped vias to form the SIW cavity structure. In the second stage, a diagonal slot is introduced within the rectangular SIW cavity to incorporate capacitance. Finally, in the last stage, additional reactive components are introduced into the structure by incorporating another diagonal slot. The combination of these slots results in a lambda (λ)-shaped slot, which further enhances the performance of the design.

Stage 1: The filtenna design begins with the selection of a rectangular SIW cavity, constructed using L-shaped vias, with two microstrip transmission lines used to feed the RF power, as depicted in Figure 6(a). The initial geometry of the proposed filtenna was determined using Eqs. (1) to (3), measuring 25 mm in length and 19 mm in width.

As observed in Figure 6(a), the feed gaps, positioned relative to the L-shaped vias, play a crucial role in regulating the external Q-factors and, consequently, ensuring proper input matching at both ports. The initial design of the SIW cavity antenna was set to operate at 11.51 GHz. The reflection coefficient and isolation of the designed antenna were analyzed, as depicted in Figure 7. With two ports considered, an isolation exceeding 10 dB was attained between them. In addition, unwanted noise and undesired frequencies were monitored and mitigated during communication.

Stage 2: The proposed antenna design initially exhibits undesired frequencies during the communication. To address this issue, the resonant frequency was adjusted to effectively mitigate unwanted noise and enhance isolation, as depicted in Figure 8.

Stage 3: Based on the isolation and reflection coefficients, all radiating slots were incorporated, and the operating frequencies of the channels were fine-tuned. The lower and upper frequency limits are depicted in Figure 9.

The final design was primarily optimized for impedance bandwidth, matching, and improved isolation. The accepted frequency ranges were 3.0% (10.61–10.93 GHz) for the lower band and 3.2% (12.19–12.59 GHz) for the upper band.

The proposed self-diplexing modified lambda (λ)-shaped antenna, along with Port 1 and Port 2, is shown in Figures 10(a) and 10(b). When both ports are active, the structure supports two pass channels: a higher resonant channel (f_U), and a lower resonant channel (f_L).

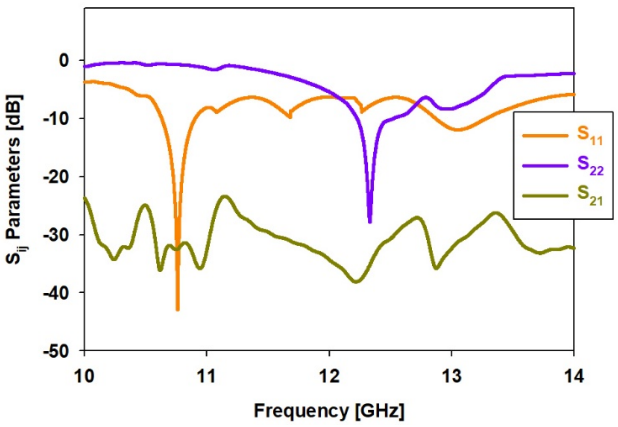

FIGURE 9. Stage 3, S_{ij} parameters.

Compared to −28 dB, the isolation between the two operational channels is significantly improved. As seen in Figure 10(a), when Port 1 is activated, radiation is emitted through the slot, with the lower frequency resonating between 10.61 GHz and 10.93 GHz, while fL maintains a passband below the −10 dB threshold. Similarly, in Figure 10(b), when Port 2 is activated, radiation is emitted through the slot, with resonances occurring between 12.19 GHz and 12.59 GHz, while the upper frequency (fU) passband remains below −10 dB. In Figures 10(a) and (b), the operating and rejected

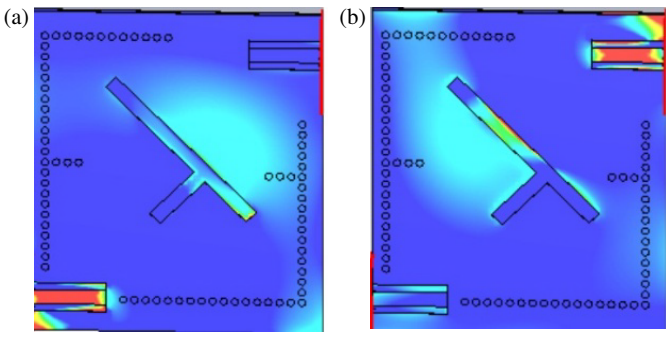

FIGURE 10. Distribution of the electric field. (a) Port-1 at 10.76 GHz. (b) Port-2 at 12.39 GHz.

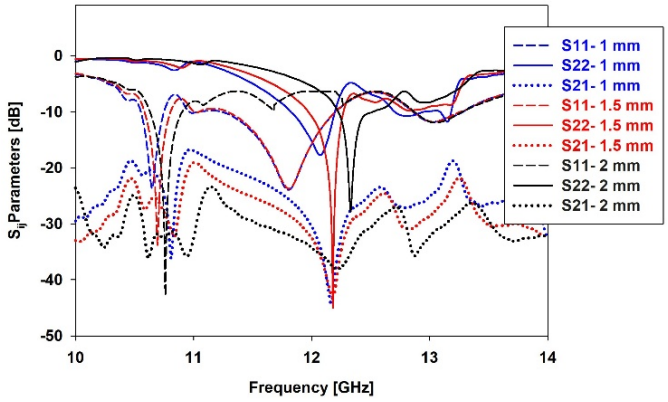

FIGURE 11. Simulated S-parameter values according to the width variation of the antenna design.

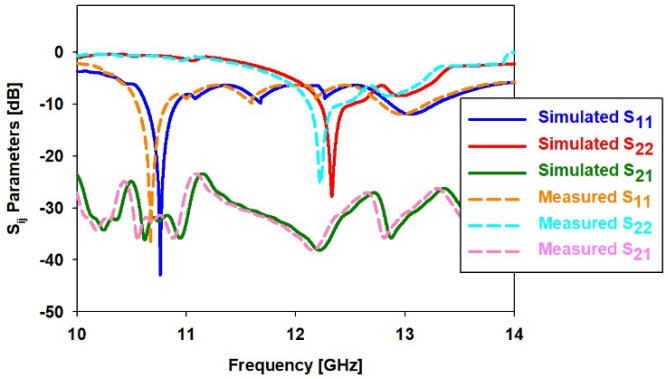

FIGURE 12. Proposed simulated and measurement results.

frequency bands are specified for excitations at Port 1 and Port 2. The results confirm self-diplexing behavior, as the excitation of one port activates its designated band while effectively suppressing the band associated with the other port.

4. PARAMETRIC ANALYSIS

Here, the impact of design variations was analyzed based on the changes in the antenna's width. The corresponding antenna specifications are illustrated in Figure 11.

The reflection coefficient values (S-parameters: S_{11}, S_{22}, S_{21} at each port, considering variations in the antenna's width, are shown in Figure 11. In this analysis, the antenna's width was varied between 1 mm and 2 mm to examine its impact on the isolation and reflection coefficients. In this investigation, varying the antenna width by 1 mm results in a resonant response at 10.45 GHz with an S_{11} of -20 dB, while a second resonance is observed at 12.01 GHz with an S_{22} of -10 dB. Increasing the antenna width to 1.5 mm produces a resonance at 10.63 GHz with an S_{11} of -33 dB, while the second resonant mode occurs at 12.21 GHz with an S_{22} of -42 dB. Finally, increasing the antenna width to 2 mm yields a resonance at 10.76 GHz with an S_{11} of -45 dB, while the second resonant mode is observed at 12.39 GHz with an S_{22} of -30 dB. This highlights the need for an optimized design to ensure the desired communication performance. The suitable frequency ranges for X-band and Ku-band applications are 10.76 GHz and 12.39 GHz, respectively. In Addition, the reflection coefficient parameter of the proposed antenna remains below -25 dB for both operating conditions.

The summary of the design phases for the suggested self-diplexing lambda (λ) shaped antenna:

Antenna Design — Implementing the SDA concept with an SIW antenna, integrating a lambda (λ)-shaped radiating slot within the specified frequency range.

Multi-Mode Cavity Development — Design a large, multi-mode SIW cavity using the CST Microwave Studio Suite electromagnetic simulator.

Impedance Matching Optimization — Adjust slot positions to improve input impedance matching.

Port Isolation — This Ensures an isolation level of 28 dB between ports.

Performance Validation — Verify the performance of the antenna for X-band and Ku-band applications.

The SIW cavity and slot configuration is interpreted as a radiation-coupled resonant system, where the dominant cavity modes act as band-pass resonators and generate inherent transmission zeros, leading to out-of-band suppression. An equivalent transfer-function-based interpretation is added to relate the resonant modes to the observed frequency-selective radiation.

5. ANTENNA TEST RESULTS AND VALIDATIONS

A prototype was fabricated and tested to verify the functionality of the proposed self-diplexing antenna. The antenna was manufactured on a dielectric slab using printed circuit board (PCB) technology, as shown in Figure 13. The top and bottom views of the fabricated antenna, including its width and length, are presented in Figures 13(a) and 13(b), respectively. A vector network analyzer was used to measure the S-parameters of the prototype. Figure 12 demonstrates the comparison between the measured and simulated S-parameters ($|S_{ij}|$). The presence of two distinct resonances confirms that the antenna operates effectively as a diplexer at both the lower and higher frequencies.

For the f_L pass channel, the measured reflection coefficient $|S_{11}|$ remains below -10 dB within a bandwidth of 3.0% (10.61–10.93 GHz). Similarly, for the f_U pass channel, the measured $|S_{22}|$ is below -10 dB with a bandwidth of 3.2% (12.19–12.59 GHz), which closely matches the simulation re-

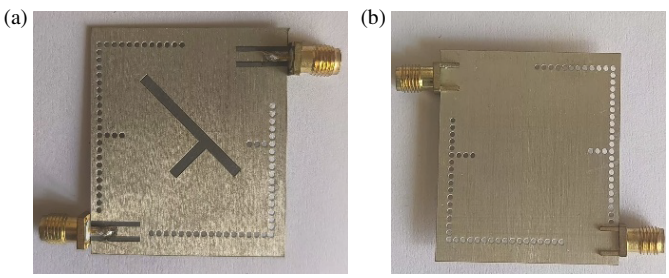

FIGURE 13. Fabricated antenna design: (a) top-side view, (b) bottom-side view.

FIGURE 14. Antenna radiation pattern and gain measurement in an anechoic chamber.

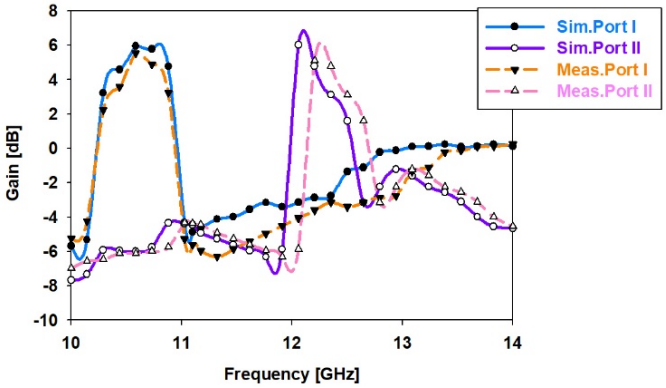

FIGURE 15. Simulation vs measurement result of gain.

sults. The observed isolation $|S_{21}|$ between Port 1 and Port 2 is displayed in Figure 12. The proposed antenna achieves improved isolation at both lower and upper frequencies, with an isolation level of -28.50 dB. Additionally, the isolation between the two resonators remains consistently above 21 dB across both the frequency bands.

Figure 13(a) presents a top view of the developed self-diplexing antenna, which features a low-profile, compact design suitable for dual-frequency applications in the X and Ku bands. The proposed antenna is constructed using a Rogers/RT 5880 substrate, adhering to industry standards for a novel self-diplexing lambda (λ)-shaped design. Figure 13(b) shows the bottom view of the substrate integrated waveguide (SIW) rectangular antenna cavity, including the vias.

Minor deviations in the resonance frequencies are associated with manufacturing and measurement tolerances. Figure 14 shows the measurement setup of the proposed antenna in an anechoic chamber. Figure 15 illustrates the gain as a function of the frequency for the proposed design, validating its diplexing properties at Port-1 and Port-2, when one port is excited and the other port terminated with a 50-Ω matched load. Owing to the proposed structure, two resonant responses are clearly observed at 10.76 GHz and 12.39 GHz. The measured gain values are 6.12 dBi and 6.15 dBi for the lower and upper frequency bands, respectively. The design exhibits a nearly flat in-band gain and provides effective stopband rejection outside the operating frequencies of 10.76 GHz and 12.39 GHz. As shown in Figure 16, the measured efficiency across the working bands exceeded 85.2%, whereas the simulated antenna efficiency reached approximately 91.16% within the -10 dB bandwidth.

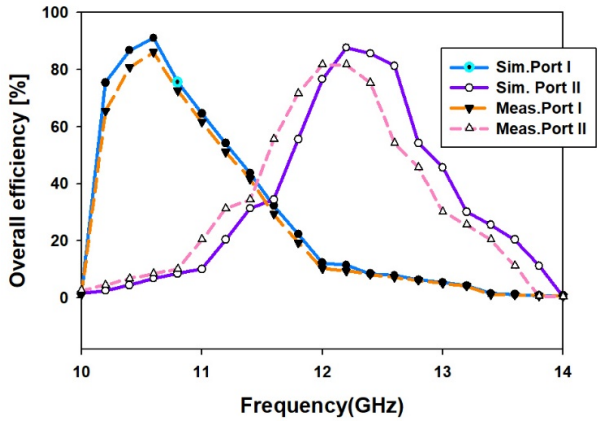

FIGURE 16. Simulation vs measurement result of total efficiency.

Figure 15 illustrates the gain analysis of the proposed self-diplexing antenna design by comparing the simulation and measurement results across different frequency values. The self-diplexing antenna achieves measured gains of 6.12 dBi and 6.15 dBi for the lower band and upper band, respectively. The design provided suitable bandwidths of 3.0% (10.61–10.93 GHz) and 3.2% (12.19–12.59 GHz), ensuring reliable performance.

Figure 16 shows the overall efficiency of the proposed substrate integrated waveguide (SIW) rectangular antenna with a lambda (λ)-shaped radiating slot. The simulated efficiency reached 91.16%, with the port isolation exceeding 28 dB. The measured efficiency remained consistently high over the operating frequency ranges, confirming the performance of the antenna for X- and Ku-band communication applications.

This section analyzes the performance of the proposed novel self-diplexing multi-mode SIW cavity antenna using a lambda (λ)-shaped radiating slot and compares it with existing antenna designs from state-of-the-art studies.

Table 1 presents a comparative analysis of the proposed self-diplexing antenna design and existing state-of-the-art diplexing antenna designs. The performance evaluation considers key parameters such as frequency, efficiency, isolation, and gain. The results indicate that the proposed self-diplexing antenna features a more compact geometry while achieving superior simulated radiation efficiency, reaching 91.16%. Overall, the findings demonstrate that the suggested design outperforms the existing antenna configurations.

The radiation patterns were evaluated through both simulations and measurements under identical conditions. During pattern measurement, one port was excited at the frequency of interest, while the other unused port was terminated with a 50-Ω matched load to avoid unwanted reflections and mutual coupling effects. The co-polarized radiation patterns were recorded in the E-plane and H-plane at the two operating frequencies, namely, Figure 17(a) E-plane co-polarization at 10.76 GHz, (b) H-plane co-polarization at 10.76 GHz, (c) E-plane co-

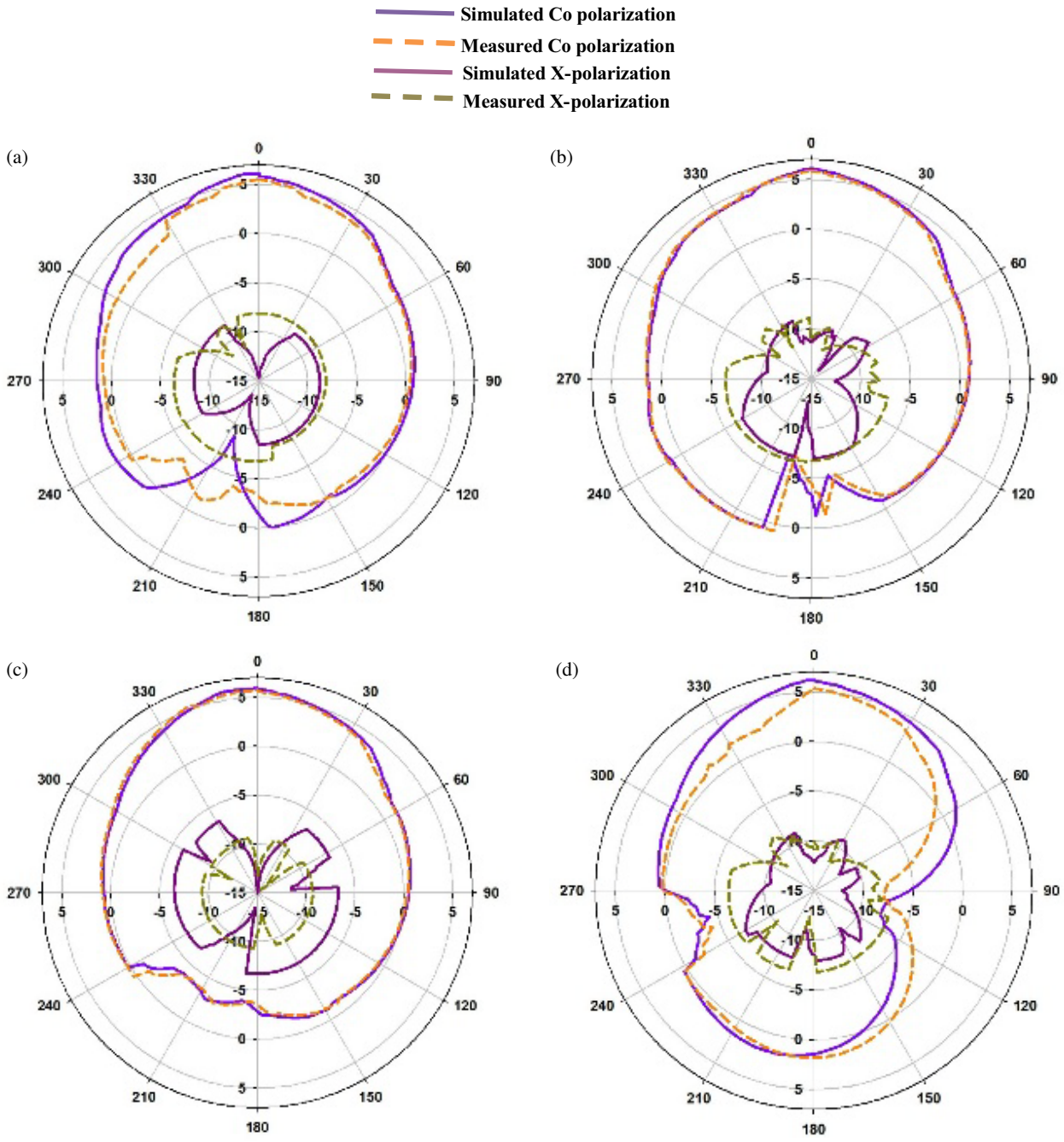

FIGURE 17. Measurements and simulations of the radiation patterns. (a) E- Co at 10.76 GHz, (b) H- Co at 10.76 GHz, (c) E- Co at 12.39 GHz and (d) H- Co at 12.39 GHz.

polarization at 12.39 GHz, and (d) H-plane co-polarization at 12.39 GHz, demonstrating good agreement between measured and simulated results.

Some minor deviations in the radiation pattern were observed owing to the cavity mode disturbances. However, the proposed antenna maintains a well-defined main lobe with co-polarization. The polarization purity is moderate, with co-polarization levels remaining below 15.0 dB in both the XZ- and YZ-planes, as confirmed by measurement data.

This work introduces an innovative self-diplexing antenna design with improved bandwidth in both passbands while maintaining comparable radiation characteristics. The hybrid modes generate two resonances in each passband, a phenomenon previously observed in SIW-based filtenna research, which often limits the realized gain. In contrast, the proposed antenna achieved a realized gain exceeding 6.0 dBi. Maintaining similar electrical behavior in both the transmission and reception channels is crucial for transceivers in all communication systems, and the proposed design effectively meets this requirement.

The proposed antenna is designed for X-band and Ku-band applications and features a novel lambda (λ)-shaped radiating slot. Existing antennas typically operate at lower frequen-

TABLE 1. Comparative analysis between the proposed and existing designed antennas by state-of-art works.

Ref.	Antenna design	Frequency (GHz)	Isolation (dB)	Gain (dBi)	Efficiency	Filtering Response	Volume (λ_o^3)
[2]	QM SIW self-diplexing antenna	3.6, 5.4	> 32.5	4.9, 5.34	NA	No	$1.3 \times 1.5 \times 0.025$
[16]	Self-diplexing slot antenna utilizing semicircular SIW structure	11.8, 12.1	22.7, 22.5	6.09, 5.87	NA	No	$1.6 \times 0.95 \times 0.03$
[18]	SIW antenna operating in eight modes	7.8, 9	>22	5.4, 5.1	NA	No	$1.3 \times 1.5 \times 0.025$
[19]	Microfluidic-enabled tunable SIW self-diplexing antenna	3.65, 5.87	> 27	5.31, 5.61	> 80.1	No	$1.19 \times 1.5 \times 0.05$
[20]	Planar Cavity-Based Filtering Antenna	4.3, 5.02	> 21	5.94,6.45	NA	Yes	$1.29 \times 1.29 \times 0.024$
[21]	Self-Diplexing Filtering Antenna for Millimeter-Wave Applications	30.5, 38.0	> 27	7.8,9.9	> 85.51	Yes	
[22]	Dual-Mode SIW Square Cavity-Based Self-Diplexing Antenna	9.5, 10.5	> 29	5.75, 5.95	NA	No	$1.18 \times 1.581 \times 0.03$
Proposed	**Self Diplexing multi mode SIW cavity back antenna based a Lambda (λ)-shaped Radiating slot**	**10.76, 12.39**	**>28**	**6.12-6.15**	**91.16%**	**Yes**	$\mathbf{1.027 \times 1.358 \times 0.0251}$

cies and suffer from limitations in key performance parameters such as isolation, gain, efficiency, and filtering characteristics. In contrast, the proposed lambda (λ)-shaped antenna supports self-diplexing operations using substrate integrated waveguide (SIW) techniques, offering enhanced performance across multiple metrics.

6. CONCLUSION

In this work, a novel lambda (λ)-shaped slot radiator based on an SIW cavity was designed and developed for filtering applications. The proposed SIW cavity antenna, featuring a lambda (λ)-shaped radiating slot, is tailored for X- and Ku-band applications, operating at 10.76 GHz and 12.39 GHz. The antenna design is optimized to achieve high performance and has been thoroughly simulated. It demonstrates excellent isolation (> 28 dB), high gain (> 6 dBi), front-to-back ratio (FTBR $>$ 10 dB), and simulated overall efficiency of 91.16% across both frequency bands. Compared with existing research, the proposed design offers enhanced performance. However, it is currently being optimized for double-band applications. In future work, this design will be extended to support wideband applications. Future work will aim to extend the antenna's bandwidth to support ultra-wideband (UWB) operation, targeting a frequency range from 1 GHz to 18 GHz. This includes exploring multi-resonant structures, broadband impedance matching techniques, and the use of metamaterial-inspired elements or slots to improve the return loss and gain over a wider frequency range. Additionally, integration with tunable or reconfigurable components should be investigated to support dynamic frequency agility in next-generation communication systems.

REFERENCES

[1] Xiang, B. J., S. Y. Zheng, H. Wong, Y. M. Pan, K. X. Wang, and M. H. Xia, "A flexible dual-band antenna with large frequency ratio and different radiation properties over the two bands," *IEEE Transactions on Antennas and Propagation*, Vol. 66, No. 2, 657–667, 2018.

[2] Iqbal, A., M. Al-Hasan, I. B. Mabrouk, and M. Nedil, "Ultracompact quarter-mode substrate integrated waveguide self-diplexing antenna," *IEEE Antennas and Wireless Propagation Letters*, Vol. 20, No. 7, 1269–1273, 2021.

[3] Asaithambi, R. and R. Kumar, "Design and implementation of novel H-shaped self-diplexing SIW rectangular cavity-backed antenna with harmonic suppression for terrestrial communications," *International Journal of Antennas and Propagation*, Vol. 2024, No. 1, 6618202, 2024.

[4] Mao, C.-X., Z. H. Jiang, D. H. Werner, S. S. Gao, and W. Hong, "Compact self-diplexing dual-band dual-sense circularly polarized array antenna with closely spaced operating frequencies," *IEEE Transactions on Antennas and Propagation*, Vol. 67, No. 7, 4617–4625, 2019.

[5] Yang, X., X. Q. Lin, B. Wang, and Y. Su, "A dual-wideband structure-shared antenna with self-diplexing property for high-power microwave application," *IEEE Transactions on Antennas and Propagation*, Vol. 69, No. 7, 4201–4205, 2021.

[6] Pandey, A. K., N. K. Sahu, R. K. Gangwar, and R. K. Chaudhary, "SIW-cavity-backed wideband circularly polarized antenna using modified split-ring slot as a radiator for mm-wave IoT applications," *IEEE Internet of Things Journal*, Vol. 11, No. 7, 11 793–11 799, 2024.

[7] Barik, R. K. and S. Koziel, "Microfluidically frequency-reconfigurable compact self-quadruplexing tunable antenna with high isolation based on substrate integrated waveguide," *Scientific Reports*, Vol. 14, No. 1, 920, 2024.

[8] Kumar, A., M. Kumar, and A. K. Singh, "On the behavior of self-triplexing SIW cavity backed antenna with non-linear replicated hybrid slot for C and X-band applications," *IEEE Access*, Vol. 10, 22 952–22 959, 2022.

[9] Kumar, A. and S. I. Rosaline, "Hybrid half-mode SIW cavity-backed diplex antenna for on-body transceiver applications," *Applied Physics A*, Vol. 127, No. 11, 834, 2021.

[10] Boukarkar, A., X. Q. Lin, Y. Jiang, and Y. Q. Yu, "A tunable dual-fed self-diplexing patch antenna," *IEEE Transactions on Antennas and Propagation*, Vol. 65, No. 6, 2874–2879, 2017.

[11] Barik, R. K., S. Koziel, Q. S. Cheng, and S. Szczepanski, "Highly miniaturized self-diplexed U-shaped slot antenna based on shielded QMSIW," *IEEE Access*, Vol. 9, 158 926–158 935, 2021.

[12] Hu, K.-Z., M.-C. Tang, Y. Wang, D. Li, and M. Li, "Compact, vertically integrated duplex filtenna with common feeding and radiating SIW cavities," *IEEE Transactions on Antennas and Propagation*, Vol. 69, No. 1, 502–507, 2021.

[13] Kumar, K., S. Priya, S. Dwari, and M. K. Mandal, "Self-quadruplexing circularly polarized SIW cavity-backed slot antennas," *IEEE Transactions on Antennas and Propagation*, Vol. 68, No. 8, 6419–6423, 2020.

[14] Lee, Y.-J., J.-H. Tarng, and S.-J. Chung, "A filtering diplexing antenna for dual-band operation with similar radiation patterns and low cross-polarization levels," *IEEE Antennas and Wireless Propagation Letters*, Vol. 16, 58–61, 2017.

[15] Iqbal, A., M. A. Selmi, L. F. Abdulrazak, O. A. Saraereh, N. K. Mallat, and A. Smida, "A compact substrate integrated waveguide cavity-backed self-triplexing antenna," *IEEE Transactions on Circuits and Systems II: Express Briefs*, Vol. 67, No. 11, 2362–2366, 2020.

[16] Agrawal, M. and T. Kumar, "A semicircular substrate integrated waveguide-based self-diplexing slot antenna with polarization flexibility," *IEEE Antennas and Wireless Propagation Letters*, Vol. 22, No. 7, 1518–1521, 2023.

[17] Lu, Y.-C. and Y.-C. Lin, "A mode-based design method for dual-band and self-diplexing antennas using double T-stubs loaded aperture," *IEEE Transactions on Antennas and Propagation*, Vol. 60, No. 12, 5596–5603, 2012.

[18] Pourmohammadi, P., H. Naseri, N. Melouki, F. Ahmed, A. Iqbal, G. A. E. Vandenbosch, and T. A. Denidni, "Substrate integrated waveguide-based full-duplex antenna with improved out-of-band suppression," *IEEE Transactions on Circuits and Systems II: Express Briefs*, Vol. 70, No. 4, 1430–1434, 2023.

[19] Pradhan, N. C., M. G. Reddy, K. S. Subramanian, R. K. Barik, S. Koziel, and Q. S. Cheng, "Microfluidic SIW-based tunable self-diplexing antenna for sub-6 GHz band applications," *IEEE Transactions on Circuits and Systems II: Express Briefs*, Vol. 70, No. 4, 1435–1439, 2023.

[20] Dhwaj, K., H. Tian, and T. Itoh, "Low-profile dual-band filtering antenna using common planar cavity," *IEEE Antennas and Wireless Propagation Letters*, Vol. 17, No. 6, 1081–1084, 2018.

[21] Xu, H., H. Liu, T. Huang, and T.-Y. Liu, "3-D-printed dual-band circularly polarized filtering antenna with self-diplexing property for millimeter-wave applications," *IEEE Transactions on Antennas and Propagation*, Vol. 72, No. 4, 3807–3812, 2024.

[22] Khan, A. A. and M. K. Mandal, "Compact self-diplexing antenna using dual-mode SIW square cavity," *IEEE Antennas and Wireless Propagation Letters*, Vol. 18, No. 2, 343–347, 2019.

[23] Bozzi, M., A. Georgiadis, and K. Wu, "Review of substrate-integrated waveguide circuits and antennas," *IET Microwaves, Antennas & Propagation*, Vol. 5, No. 8, 909–920, 2011.

[24] Xu, F. and K. Wu, "Guided-wave and leakage characteristics of substrate integrated waveguide," *IEEE Transactions on Microwave Theory and Techniques*, Vol. 53, No. 1, 66–73, 2005.

[25] Pradhan, N. C., K. S. Subramanian, R. K. Barik, and Q. S. Cheng, "A shielded-QMSIW-based self-diplexing antenna for closely spaced bands and high isolation," *IEEE Antennas and Wireless Propagation Letters*, Vol. 20, No. 12, 2382–2386, 2021.

[26] Jin, C., R. Li, A. Alphones, and X. Bao, "Quarter-mode substrate integrated waveguide and its application to antennas design," *IEEE Transactions on Antennas and Propagation*, Vol. 61, No. 6, 2921–2928, 2013.